ASTRONOMY & ASTROPHYSICS
SUPPLEMENT SERIES

Astron. Astrophys. Suppl. Ser. **139**, 173–177 (1999)

Integrated optics for astronomical interferometry

II. First laboratory white-light interferograms

J.P. Berger[1], K. Rousselet-Perraut[1], P. Kern[1], F. Malbet[1], I. Schanen-Duport[2], F. Reynaud[3], P. Haguenauer[1,4], and P. Benech[2]

[1] Laboratoire d'Astrophysique UMR CNRS/UJF 5571, Observatoire de Grenoble, BP. 53, F-38041 Grenoble Cedex 9, France
[2] Laboratoire d'Électromagnétisme Microondes et Optoélectronique UMR CNRS/INPG/UJF 5530, BP. 257, F-38016 Grenoble Cedex 1, France
[3] Institut de Recherche en Communications Optiques et Microondes, UMR CNRS/Univ. Limoges 6615, 123 avenue Albert Thomas, F-87060 Limoges Cedex, France
[4] CSO Mesures 70, Avenue des Martyrs, F-38000 Grenoble, France

Received February 25; accepted June 4, 1999

Abstract. We report first white-light interferograms obtained with an integrated optics beam combiner on a glass plate. These results demonstrate the feasability of single-mode interferometric beam combination with integrated optics technology presented and discussed in Paper I (Malbet et al. 1999). The demonstration is achieved in laboratory with off-the-shelves components coming from micro-sensor applications, not optimized for astronomical use. These two-telescope beam combiners made by ion exchange technique on glass substrate provide laboratory white-light interferograms simultaneously with photometric calibration. A dedicated interferometric workbench using optical fibers is set up to characterize these devices. Despite the rather low match of the component parameters to astronomical constraints, we obtain stable contrasts higher than 93% with a 1.54-μm laser source and up to 78% with a white-light source in the astronomical H band. Global throughput of 27% for a potassium ion exchange beam combiner and of 43% for a silver one are reached. This work validates our approach for combining several stellar beams of a long baseline interferometer with integrated optics components.

Key words: instrumentation, astronomical interferometry, integrated optics

Send offprint requests to: J.P. Berger
Correspondence to: berger,malbet@obs.ujf-grenoble.fr

1. Introduction

Since Froehly (1981) proposed guided optics for astronomical interferometry, important progress has been made. In particular, the FLUOR instrument which combines two interferometric beams with single-mode fiber couplers (Coudé du Foresto 1994) has led to astrophysical results with unprecedent precision. This experiment demonstrated the great interest of spatial filtering combined with photometric calibration to improve the visibility accuracy. More recently, Kern et al. (1996) suggested to combine interferometric beams with integrated optics components since this technology allows to manufacture single-mode waveguides in a planar substrate. In Paper I (Malbet et al. 1999), we presented and discussed thoroughly the advantages and limitations of integrated optics for astronomical interferometry. To validate the latter analysis, we have performed several laboratory experiments with existing components not optimized for interferometry but allowing to get first clues on this technology. The first experimental results are reported in this paper.

2. Experimental set-up

We carried out laboratory tests with off-the-shelves integrated optics components designed for micro-sensor applications. The waveguides are made by ion exchange (here potassium or silver) on a standard glass substrate thanks to photolithography techniques (Schanen-Duport et al. 1996). The exchanged area is analogous to the core of an optical fiber and the glass substrate to the fiber cladding. Our 5 mm $\times$ 40 mm component is schematically

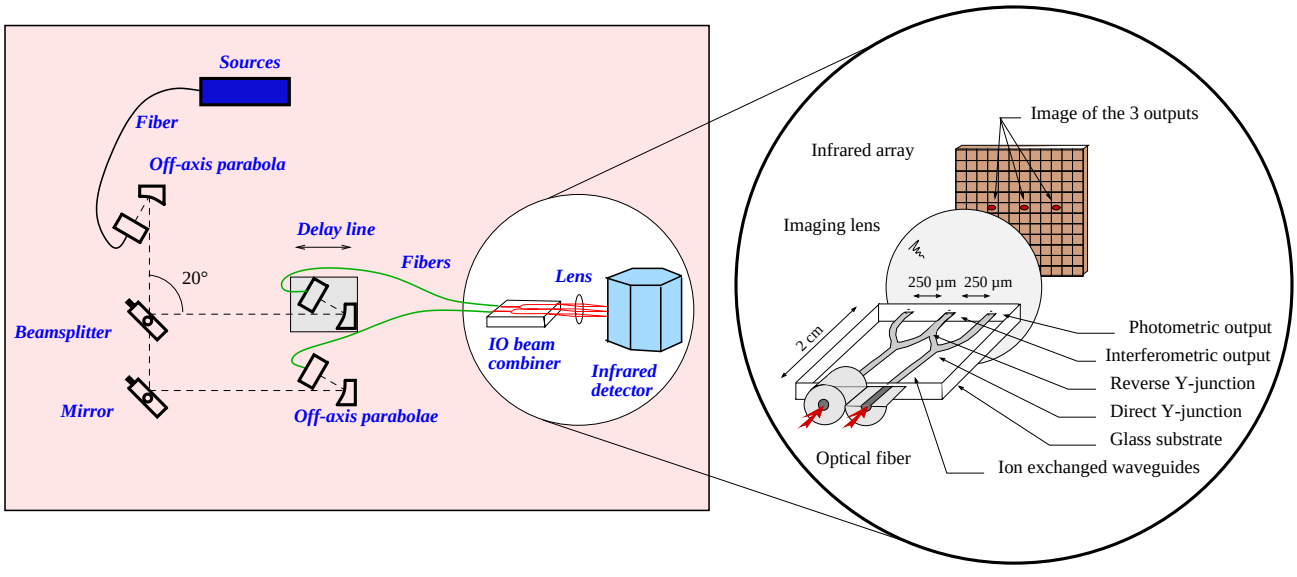

Fig. 1. Left: laboratory interferometric workbench for testing integrated optics beam combiners based on a Mach-Zehnder interferometer concept. The collimated beam provided by the sources (laser, laser diode or white-light source) is splitted in two beams which are focused onto low-birefringence single-mode fibers by off-axis parabolae. Fibers are directly connected to the integrated optics beam combiner. The optical path difference between the beams is modulated by a translating stage to produce a delay. The three outputs of the beam combiner are imaged on a cooled infrared HgCdTe array. The angle between the incident and reflected beams on the beamsplitter is close to 20°. Right: integrated optics two-way beam combiner. The light from the telescopes is coupled into the integrated optics beam combiner thanks to optical fibers. Two direct Y-junctions provide photometric calibration signals for each beam. A reverse Y-junction combines the two input beams. Each output is imaged by a lens onto an infrared array

depicted in the right part of Fig. 1. We use it as a two-way beam combiner with two photometric calibration signals. The component operates in the H atmospheric band (1.43 μm − 1.77 μm) and its waveguides are single-mode in that domain. From an optical point of view, the reverse Y-junction acts as one of the two outputs of a classical beam splitter. The second part of the interferometric signal with a π phase shift is radiated at large scale in the substrate. Light is carried to the component thanks to standard non-birefringent silica fibers.

We have set up a laboratory Mach-Zehnder interferometer to test the interferometric capabilities of our components (see the left part of Fig. 1). The available sources are: a 1.54-μm He-Ne laser, a 1.55-μm laser diode and an halogen white-light source. The latter is used with an astronomical H filter.

We scan the interferograms by modulating the optical path difference (OPD) with four points per fringe. The delay line speed is restricted by the integration time (∼1 ms for laser sources and ∼10 ms for the white-light source to get a sufficient signal-to-noise ratio) and the frame rate (50 ms of read-out time for the full frame). The OPD scan and the data acquisition are not synchronized, but for each image the translating stage provides a position with an accuracy of 0.3 μm . The simultaneous recording of the photometric and interferometric signals allows to unbias the fringe contrast from the photometric fluctuations as suggested by Connes et al. (1984) and validated by Coudé du Foresto (1994).

A typical white light interferogram I_0 is plotted in Fig. 2a together with the simultaneous photometric signals P_1 and P_2. To correct the raw interferogram from the photometric fluctuations, we substract a linear combination of P_1 and P_2 from I_0. The expression of the corrected interferogram is then

$$I_c = \frac{I_0 - \alpha P_1 - \beta P_2}{2\sqrt{\alpha P_1 \, \beta P_2}} \quad (1)$$

with α and β coefficients determined by occulting alternatively each input beam. The resulting corrected interferogram is displayed in Fig. 2b.

3. Results and discussion

As far as an astronomer is concerned, the physical quantities of interest when dealing with an interferometric instrument are the instrumental contrast, the optical stability, and the total optical throughput.

3.1. Laser-light constrasts

A 93% contrast is obtained with the He-Ne laser. The main source of contrast variations with time comes from

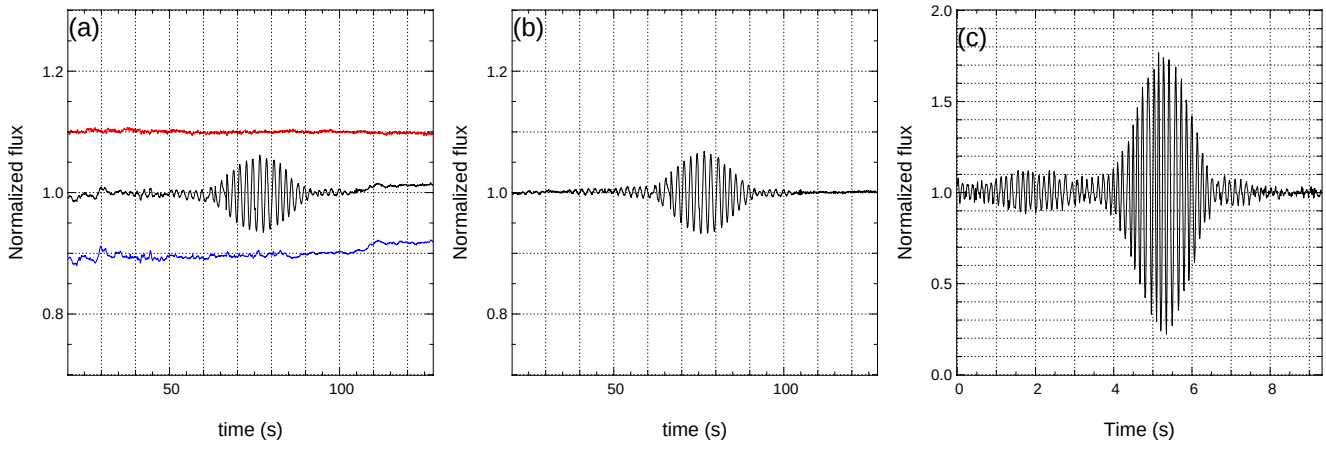

Fig. 2. White-light interferograms obtained in laboratory with integrated optics components: potassium ion exchange component connected with low-birefringent fibers **a**, **b)** and silver ion exchange component connected with high-birefringent fibers **c)**. **a)** Raw interferogram in the H atmospheric band with photometric calibration signals (upper and lower curves with vertical shifts of +0.1 and −0.1) in normalized units. **b)** Interferogram corrected from the photometry **b)** in same units. **c)** Photometry-corrected interferogram obtained with input beams polarized along the neutral axis of high-birefringent fibers

temperature gradient and mechanical constraints on the input fibers. When special care is taken to avoid fiber bending and twists, the laser contrast variation is lower than 7% rms over a week. Using high-birefringent fibers which are far less sensitive to mechanical stresses will improve the contrast stability.

3.2. White-light contrasts

With an halogen white-light source, the contrast obtained is of the order of 7% with a potassium ion beam combiner connected with low-birefringent fibers (Fig. 2b) and 78% with a silver ion beam combiner connected with high-birefringent fibers (Fig. 2c). Two main sources of interferometric contrast drops between the two components have been identified: chromatic dispersion and polarization mismatch.

The consequence of residual differential dispersion between the two arms is to spread out the fringe envelope and decrease the contrast. Since the delay line translation is not perfectly linear, the Fourier relation between space and time is affected and an accurate estimate of the dispersion is difficult. Only the number of fringes and the shape of the interferogram gives an idea of the existing differential dispersion. The theoretical number of fringes is given by the formula $2\frac{\lambda}{\Delta\lambda} \sim 10$ and the interferogram contains about 13 fringes. Such a spread is not sufficient to explain the contrast drop between the laser- and white-light interferograms. More detailed studies of residual chromatic dispersion are in progress.

In the present case the contrast decay is mainly explained by differential birefringence. Low-birefringent fibers are known to be highly sensitive to mechanical constraints and temperature changes, leading to unpredictable birefringence. Coupling between polarisation

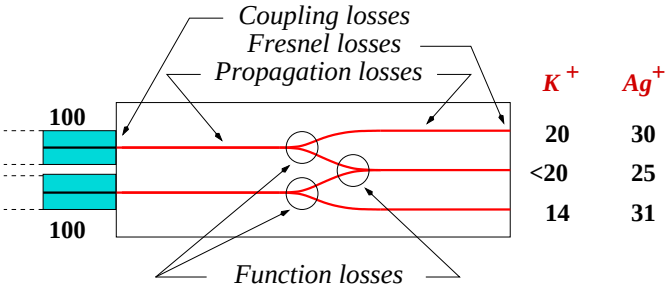

Fig. 3. Schematic view of the beam combiner with successives optical losses (see text for details). Number of output photons are given for 100 incoherent photons injected in each channel for potassium- and silver-exchanged waveguides

modes can occur leading to a contrast loss which can be worse for unpolarized incident light (case of the thermal white-light source). This is confirmed by the preliminary results obtained with high-birefringent fibers and the incident light polarized along the neutral axes: the contrast reaches 78% (Fig. 2c). The apparent asymmetry of the interferogram could be due to residual differential polarization and/or dispersion. Full characterizations are in progress and will be reported in Paper III (Haguenauer et al. 1999).

3.3. Total throughput

Figure 3 summarizes the photon losses in the two components. We express the losses in terms of remaining photons when 100 *incoherent* photons are injected at each waveguide input. For the component made from potassium ion exchange, we obtain 20 and 14 photons on each photometric channel and less than 20 photons in the interferometric channel leading to a total of 54 photons for 200 photons

Table 1. Estimation of optical losses at different levels of fiber-connected beam combiners with respectively potassium- and silver-exchanged waveguides. The number of detected and estimated output photons are given for our 4-cm components. Last column gives an idea of what performances can be achieved in the future

Component	K^+	Ag^+	*Future*
Fiber/waveguide coupling	40%	20%	*4.5%*
Propagation[a]	24%	9%	*9%*
Function	10%	10%	*5%*
Fresnel reflexion	4%	4%	-
Beam combination[b]	50%	50%	-
Number of input photons	200	200	-
Detected photons	54	86	-
Experimental throughput	27%	43%	-
Theoretical throughput	28%	46%	*74%*

[a] K^+: 0.3 dB/cm, Ag^+: 0.1 dB/cm for a total length of 4 cm.

[b] 50% of the flux in a reverse Y-junction is radiated out in the substrate (see Paper I).

injected, hence a total throughput of 27%. For silver ion exchange, respectively 30, 31 and 25 photons have been measured leading to a throughput of 43%. The main difference between the two results comes from the coupling efficiency between the fiber and the waveguides and the propagation losses.

Table 1 summarizes estimation of losses coming from different origins. The propagation losses and the coupling losses have been measured with a straight waveguide manufactured in the same conditions. The Fresnel losses have been theoretically estimated to 4%. Any function causes additional losses which cannot be evaluated separately but have been estimated to 10%. One should notice that the reverse Y-junction acts as only one of the two outputs of an optical beamsplitter (see Paper I). Therefore 50% of the light is radiated outside the waveguide. The first two columns of Table 1 show that our measurements are consistent with the theoretical performances computed from the different optical losses reported in the table.

Last column of Table 1 gives an order of magnitude of expected improvement in the future. The main progress concerns the beam combination function. We should be able to retrieve the second half of the combined photons thanks to new combination schemes like X-couplers, multiaxial beam combiners or multimode interferometric (MMI) multiplexers (see Paper I) at the cost of a slight chromaticity of the function. Some components including these new functions are being manufactured and will be soon tested. The ultimate optical throughput would be around $70-80\%$, twice more than our current results.

4. Conclusion and future prospects

We have obtained first high-contrast white-light interferograms with an off-the-shelves integrated optics component used as a two aperture beam combiner. The high and stable contrasts as well as the high optical throughput validate our approach for combining stellar beams by means of integrated optics presented in Paper I.

This preliminary analysis requires further characterizations and improvements. The importance of dispersion, birefringence and other phenomena in the fibers and in the components have to be fully understood. For this purpose, two-way beam combiners optimized for astronomy are under characterization (spectroscopic and polarimetric measurements for instance) in order to carefully control their optical properties. A complete description of optical and interferometric properties of integrated optics component will be presented in a forthcoming Paper (Haguenauer et al. 1999). The optical fibers should maintain polarization to avoid specific contrast losses and have optimized lengths to avoid chromatic dispersion. This experimental precaution is decisive to achieve image reconstruction (Delage 1998).

Our research program is based on the study of new integrated optics technologies for long baseline interferometry in the infrared, and, the design of beam combiners for multiple apertures[1] (see Paper I). Some specific beam combiners will then be eventually used in a scientific instrumental prototype on astronomical interferometers. Preliminary tests on the GI2T/Regain interferometer (Mourard et al. 1998) will be carried out with the Integrated Optics Near-infrared Interferometric Camera (IONIC) prototype (Berger et al. 1998).

Acknowledgements. We would like to warmly thank E. Le Coarer for his precious support in instrument control. We thank the referee, Dr. Shaklan, for a careful reading of our paper and for suggestions which helped to improve its content. The work was partially funded by PNHRA/INSU, CNRS/Ultimatech and DGA/DRET (Contract 971091). The integrated optics components have been manufactured and fiber-connected by the GeeO company.

References

Berger J.P., Rousselet-Perraut K., Kern P., et al., 1998, Proc. SPIE 3350, 898

Connes P., Froehly C., Facq P., 1984, A Fiber-Linked Version of Project TRIO, in: Longdon N., Melita O. (eds.) Proc. ESA Colloq., Kilometric Optical Arrays in Space. ESA, Cargèse, p. 49

Coudé du Foresto V., 1994, Ph.D. Thesis, Université de Paris, France

Coudé du Foresto V., Ridgway S., Mariotti J.M., 1997, A&AS 121, 379

[1] Actually 3-way and 4-way beam combiners have already been manufactured.

Delage L., 1998, Ph.D. Thesis, Université de Limoges, France
Froehly C., 1981, Coherence and Interferometry through Optical Fibers, in: Ulrich M.H., Kjär K. (eds.) Proc. ESO Conf., Science Importance of High Angular Resolution at Infrared and Optical Wavelengths. ESO, Garching, p. 285
Kern P., Malbet F., Schanen-Duport I., Benech P., 1996, Integrated optics single-mode interferometric beam combiner for near infrared astronomy, in: Kern P., Malbet F. (eds.) Proc. AstroFib'96, Integrated Optics for Astronomical Interferometry. Bastianelli-Guirimand, Grenoble, p. 195
Haguenauer P., et al., 1999 (in preparation)
Lagorceix H., 1995, Ph.D. Thesis, Université de Limoges, France
Malbet F., Kern P., Schanen-Duport I., et al., 1998, A&AS 138, 135 (Paper I)
Mourard D., et al., 1998, SPIE Proc. 3350, 517
Schanen-Duport I., Benech P., Kern P., Malbet F., 1996, Optical Waveguides Made by Ion Exchange for Astronomical Interferometry Applications at the Wavelength of 2.2 Microns. In: Kern P., Malbet F. (eds.) Proc. AstroFib'96, Integrated Optics for Astronomical Interferometry. Bastianelli-Guirimand, Grenoble, p. 99